AGU PUBLICATIONS

JGR

Journal of Geophysical Research: Oceans

RESEARCH ARTICLE

10.1002/2015JC011082

Key Points:

- Ocean surface currents are influenced by surface waves
- Surface currents considering the impact of waves are better adapted to drifter currents
- The impact of waves on currents is especially obvious in the Southern Ocean region

Correspondence to:
Y. Xu,
yongsheng.xu@qdio.ac.cn

Citation:
Hui, Z., and Y. Xu (2016), The impact of wave-induced Coriolis-Stokes forcing on satellite-derived ocean surface currents, *J. Geophys. Res. Oceans*, *121*, 410–426, doi:10.1002/2015JC011082.

Received 6 JUL 2015
Accepted 8 DEC 2015
Accepted article online 14 DEC 2015
Published online 11 JAN 2016

Corrected 10 FEB 2016
This article was corrected on 10 FEB 2016. See the end of the full text for details.

The impact of wave-induced Coriolis-Stokes forcing on satellite-derived ocean surface currents

Zhenli Hui[1,2,3] and Yongsheng Xu[1,2]

[1]Key Laboratory of Ocean Circulation and Waves, Institute of Oceanology, Chinese Academy of Sciences, Qingdao, China, [2]Laboratory for Ocean and Climate Dynamics, Qingdao National Laboratory for Marine Science and Technology, Qingdao, China, [3]University of Chinese Academy of Sciences, Beijing, China

Abstract Ocean surface currents estimated from the satellite data consist of two terms: Ekman currents from the wind stress and geostrophic currents from the sea surface height (SSH). But the classical Ekman model does not consider the wave effects. By taking the wave-induced Coriolis-Stokes forcing into account, the impact of waves (primarily the Stokes drift) on ocean surface currents is investigated and the wave-modified currents are formed. The products are validated by comparing with OSCAR currents and Lagrangian drifter velocity. The result shows that our products with the Stokes drift are better adapted to the in situ Lagrangian drifter currents. Especially in the Southern Ocean region (40°S–65°S), 90% (91%) of the zonal (meridional) currents have been improved compared with currents that do not include Stokes drift. The correlation (RMSE) in the Southern Ocean has also increased (decreased) from 0.78 (13) to 0.81 (10.99) for the zonal component and 0.76 (10.87) to 0.79 (10.09) for the meridional component. This finding provides the evidence that waves indeed play an important role in the ocean circulation, and need to be represented in numerical simulations of the global ocean circulation.

1. Introduction

Ocean surface currents are of great importance for climate studies and have received increasing attention by researchers and marine forecasters in recent years. They are the main transporters of ocean heat, salt, and chlorophyll [*Sikhakolli et al*., 2013]. Traditional currents have been acquired from ships, floating buoys, and moored current meters [*Sikhakolli et al*., 2013], which have very limited observations and coarse spatial resolutions. In recent years, oceanic remote sensing have achieved rapid development, which have very high temporal and spatial resolutions and can measure sea level anomaly (SLA), sea surface wind (SSW), and sea surface temperature (SST) conveniently under all weather conditions. Yet there is no sensor to measure ocean surface currents directly up to now [*Sikhakolli et al*., 2013]. Therefore, combining satellite data with dynamics method is an important route to acquire surface currents on large spatial scales. *Lagerloef et al*. [1999] proposed a two parameter model, in which geostrophic currents and Ekman currents were assumed to account for the lowest-order dynamics of the surface velocity and can be obtained independently from SSH and wind stress data. *Sudre and Morrow* [2008] and *Sudre et al*. [2013] used the same method to retrieve the 0.5° × 0.5° ocean surface currents of the global ocean and conclude that the sea surface flow estimated from the satellite remote sensing data can describe the real-world ocean flow objectively and accurately. Furthermore, *Bonjean and Lagerloef* [2002] devised an algorithm especially aiming at tropical Pacific which takes sea surface temperature into account. The product is known to be the Ocean Surface Current Analysis Real-time (OSCAR) and has been validated by *Johnson et al*. [2007] successfully.

In spite of this, it is not totally successful as some observational evidence does not directly support the classical Ekman model in the following features [*Lewis and Belcher*, 2004; *Polton et al*., 2005; *Price and Sundermeyer*, 1999; *Song*, 2009; *Wu and Liu*, 2008]. *Huang* [1979] believed that the Ekman current lies at an angle of between 10° and 45° to the wind stress. *Cushman-Roisin* [1994] got a smaller angle ranging from 5° to 10°. *Price and Sundermeyer* [1999] pointed out that the current deflected approximately 75° from the wind stress at a depth between 5 and 20 m and attenuated rapidly below the surface, all of which are not consistent with the predicted 45°. In order to solve the drawbacks, the classical Ekman current has to be modified. Up till now, ocean surface waves have long been known to give rise to near-surface drift currents, which can change the nature of the Ekman layer qualitatively and determine the wind-driven current profile.

Some researchers have already studied the effects of waves on the ocean circulation. For example, *Huang* [1979] indicated that Ekman currents can be generated by both the direct wind stress in the classical Ekman model and the Stokes drift from the surface wave motion. *Perrie et al*. [2003] studied the impact of waves on surface currents, who indicated that the wave-modified currents can exceed usual Ekman currents by almost 40% for rapidly developing intense storms. A study of wave effects on surface currents on the Grand Banks was carried out by *Tang et al*. [2007], who noted that the inclusion of wave effects can improve the model simulations significantly. *Song* [2009] studied the effects of random surface waves on the steady Ekman current both under eddy viscosity independent of depth and increasing linearly with depth, he concluded that Ekman currents are significantly influenced by surface waves. *Liu et al.* [2007] and *Wu and Liu* [2008] incorporated the Coriolis-Stokes forcing into the classical Ekman model and investigated the energy input to the Ekman-Stokes layer, they found that the wave-induced energy input to the Ekman-Stokes layer accounts for 12% of the total energy input of the global ocean, while the percentage increases to 22% in the Antarctic Circumpolar Current (ACC). *Song* [2009], *Perrie et al*. [2003], and *Tang et al*. [2007] indicated that the Stokes drift, wind input, and wave dissipation are all the elements of wave effects on surface currents, wind input energy to waves, and wave energy dissipation converted to currents. However, *Song* [2009] pointed out that the effects of wind input and wave dissipation on Ekman currents are small, relative to the impacts of Stokes drift, which is defined as the mean velocity of fluid particles over a wave cycle. From the papers of *Perrie et al*. [2003] and *Tang et al*. [2007], we can also conclude that in rapidly developing intense storms, wave-modified currents can exceed the classical Ekman currents by as much as 40% and a large part of this increase can be attributed to the Stokes drift. In this study, we ignore the effects of wind input and wave dissipation and only consider the Stokes drift. According to *Stokes* [1847], Stokes drift is a ubiquitous phenomenon on the sea surface, which is a mean Lagrangian flow produced by the surface wave and the direction is in accord with wave propagation [*Liu et al*., 2007]. *Hasselmann* [1970] noted that the interaction between planetary vorticity and the Stokes drift yields a Coriolis-Stokes forcing, which may have a great impact on the classical Ekman model. By incorporating the Coriolis-Stokes forcing into the momentum balance of the Ekman layer, both *Polton et al*. [2005] and *Lewis and Belcher* [2004] have pointed out that the Ekman-Stokes model agrees much better with observations than the classical Ekman model. As the Ekman current constitutes an important part of the surface current, we predict that surface waves will affect the surface current as well. Nevertheless, the previous works are either from the perspective of complicated ocean models or the study of wave effects on classical Ekman currents. The wave data used above are mostly from wavenumber spectrum. However, no one has studied the impact of waves on ocean surface currents estimated from the satellite remote sensing data and the calculation of Stokes drift using ECMWF Interim surface wave data has not been done before either.

The paper intends to estimate the satellite-derived ocean surface currents considering the impact of Stokes drift, with an emphasis on how the surface wave could affect surface currents. We construct a simple wave-affected Ekman model which has already been used by several authors like *Lewis and Belcher* [2004], *Liu et al*. [2007], *McWilliams and Restrepo* [1999], *Polton et al*. [2005], and *Wu and Liu* [2008]. Then the products are validated by comparing with OSCAR currents and in situ observations. Four kinds of products are formed in the text while comparing with in situ data, the classical ocean surface currents (without waves), wave-modified products, OSCAR currents (directly downloaded from OSCAR website), and wave-modified OSCAR currents.

The paper is organized as follows. Section 2 lists the data sets we used in this paper. In section 3, we describe the method we use to calculate each part of the ocean surface currents detailedly. Section 4 gives our results and analysis. Finally, section 5 presents the summary and conclusions.

2. Data and Processing

2.1. Wind Stress, Wind Speed, Sea Surface Height, and Sea Surface Wave Data

All the data sets used in this paper are spanning 9 years from 1 January 2000 to 31 December 2008. Wind speed, wind stress, and SSH data are from the satellite observations. For example, QuikSCAT was launched by the National Aeronautics and Space Administration (NASA; http://winds.jpl.nasa.gov/missions/quikscat/index.cfm) on 19 June 1999. The mission has a daily coverage over 92% of the global ice-free oceans and measures the wind stress and direction under all weather conditions. We use its mean wind field global 1/4° resolution product, which provides daily wind speed and stress fields and is processed and distributed by the Centre ERS d'Archivage et de Traitement (CERSAT; http://cersat.ifremer.fr/). The daily wind stress data sets are used to retrieve the classical Ekman currents of the global ocean. The global daily averaged SSH data are provided by the French Space Agency, Archiving, Validation, and Interpretation of Satellite Oceanographic Data (AVISO; http://aviso.altimetry.fr/index.php?id=1271). The 1/4° gridded MADT product for the current period merges up to four satellites (TOPEX/Poseidon, Jason-1, ERS-1/2, Envisat and so on) available at a given time. The SSH gradients are then used for computation of geostrophic currents. In this paper, the European Center for Medium-Range Weather Forecasts (ECMWF; http://apps.ecmwf.int/datasets/) Interim sea surface wave data (http://apps.ecmwf.int/datasets/data/interim-full-daily), which contains three variables listed as mean wave direction, mean wave period, and significant wave height, together with QuikSCAT wind speed, are used to calculate the Stokes drift and the wave-modified term. The global data are sampled every 6 h and are on a 0.75° $\times$ 0.75° latitude-longitude grid. As the spatial and temporal resolutions of the surface wave data are not identical to the wind stress and SSH ones, here the ECMWF data are temporally averaged and spatially interpolated to match the QuikSCAT and Aviso data's times and positions.

2.2. OSCAR

The Ocean Surface Current Analyses Real-Time (OSCAR; http://www.oscar.noaa.gov/) data we used are obtained from the NASA Physical Oceanography DAAC (http://podaac.jpl.nasa.gov/) and developed by ESR, which provides unfiltered gridded ocean surface current information with a spatial resolution of 1/3° and temporal resolution of 5 days, whose deriving method is based on the quasi-steady and quasi-linear momentum equations, neglecting local acceleration [*Bonjean and Lagerloef*, 2002]. This product is directly constructed from the SSH, scatterometer winds, and both Advanced Very High Resolution Radiometer (AVHRR) and sea surface temperatures (SST) from *Reynolds et al*. [2002] to acquire global surface currents [*Bonjean and Lagerloef*, 2002; *Johnson et al*., 2007; *Liu et al*., 2014]. Both SSH and scatterometer winds data are collected during ongoing satellite missions since October 1992. Aviso MADT fields are used from 1992 to the present day. The scatterometer wind is provided by the variational analysis Special Sensor Microwave Imager (SSM/I) winds for the period October 1992 to July 1999 [*Atlas et al*., 1996], QuikSCAT gridded winds for its full run (1999–2009), ERA interim winds are used after QuikSCAT, and then NCEP for near-real time. In this paper, the OSCAR product, added with the wave-modified term, can be used to compare directly with our results on a global scale.

2.3. Global Lagrangian Drifter Data

In situ Lagrangian drifter data from the Global Drifter Program (GDP; http://www.aoml.noaa.gov/phod/dac/index.php) are used to validate the satellite-derived ocean surface currents in the analysis. The difference is that drifter motion itself is the Lagrangian velocity which already contains the wave motion, while ocean surface currents estimated from the satellite SSH and the surface wind stress are just the quasi-Eulerian velocity, which is equal to the Lagrangian mean current minus the Stokes drift and can be understood as the Eulerian mean currents as stated by *Jenkins* [1987] and *Jenkins* [1989]. The drifter data provide zonal and meridional near-surface current observations from the satellite-tracked drifters that have a drogue centered at a depth of 15 m to reduce the downwind slip to $\sim$0.1% of the wind speed for winds up to 10 m/s [*Lumpkin and Pazos*, 2007; *Niiler and Paduan*, 1995]. When this drogue is lost, the downwind slip increases to $\sim$1–1.5% of the wind speed [*Pazan and Niiler*, 2001]. In this paper, we have removed undrogued data and only the drifter data with drogues on are used. For the period between 2000 and 2008, we collect 5401 floating buoys in total. We use 9,229,932 profiles from these data sets over the global ocean. Unlike the gridded data described above, drifter observations are not in grids and are distributed irregularly. The drifter locations are shown in Figure 1a. Figure 1b shows histogram of Lagrangian drifters available in each month from January 2000 to December 2008. Furthermore, the number of drifters within any 1 year is in the range from 386 to 2159. For a single drifter, the longest lasted for 2356 days from 1 January 2000 to 13 June 2006 nonstop. The drifter data are quality controlled and have been interpolated via kriging to regular 6 h intervals [*Hansen and Poulain*, 1996].

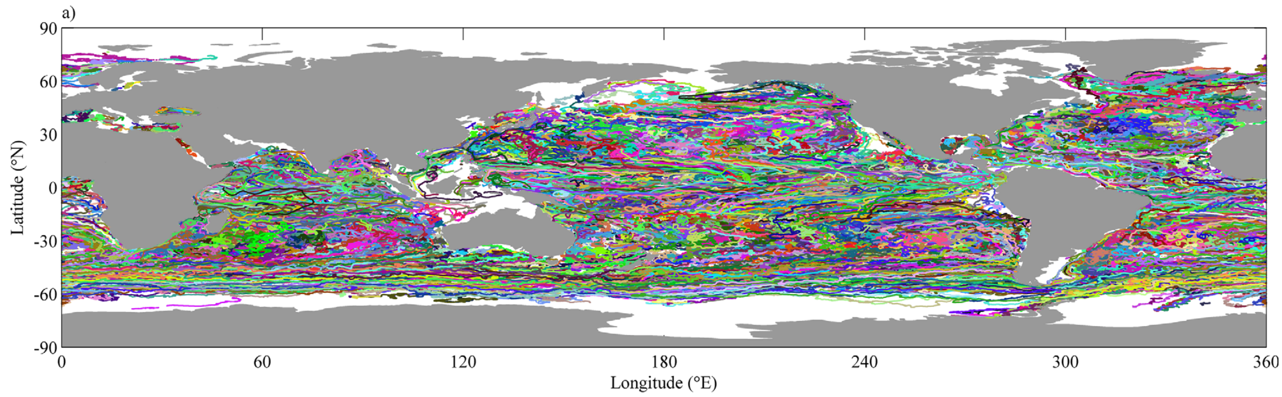

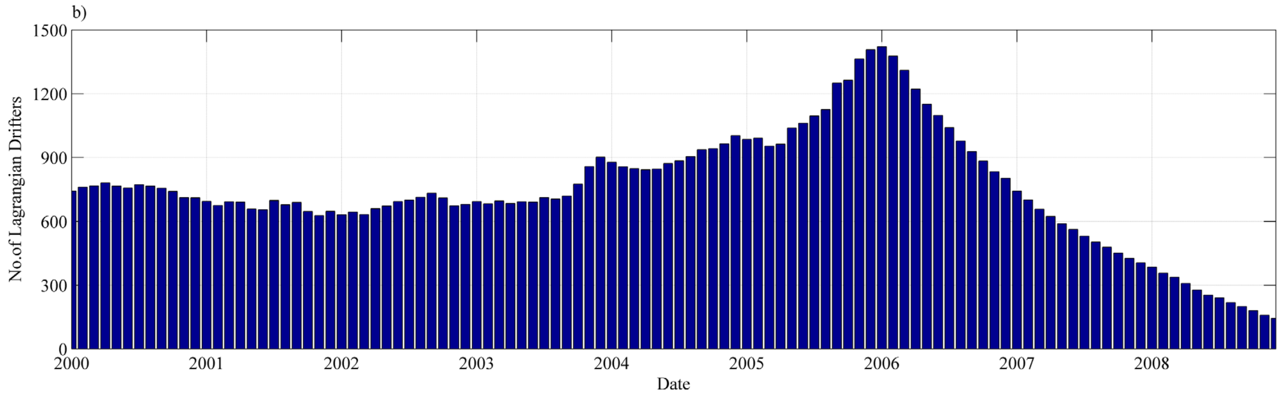

Figure 1. (a) Trajectories of the GDP Lagrangian drifters for the global ocean used to validate the satellite-derived ocean surface currents. (b) Histogram of Lagrangian drifters available in each month from January 2000 to December 2008.

3. Methods

3.1. Equations of Motion

According to *Lagerloef et al*. [1999], ocean surface currents retrieved from the satellite remote sensing data, which include geostrophic currents $\boldsymbol{U}_g$ from the SSH and Ekman currents $\boldsymbol{U}_e$ from the sea surface stress can represent the motion of standard 15 m drogue drifters. The method can be expressed as $\boldsymbol{U}_c=\boldsymbol{U}_g+\boldsymbol{U}_e$. However, $\boldsymbol{U}_c$ refers to the classical currents which means that it does not consider the effects of surface waves. As we know, surface waves can produce a mean Lagrangian transport in their direction of propagation known as the Stokes drift [*Polton et al*., 2005]. In this paper, we use the wave-modified equations which include the Stokes drift $\boldsymbol{U}_s$ in the motion. Then, the wave-modified ocean surface currents can be regarded as the sum of geostrophic currents $\boldsymbol{U}_g$, classical Ekman currents $\boldsymbol{U}_e$ and the wave-modified term $\boldsymbol{U}_w$, which is related with the Stokes drift $\boldsymbol{U}_s$, namely

$$\boldsymbol{U}=(u,v)=\boldsymbol{U}_c+\boldsymbol{U}_w=\boldsymbol{U}_g+\boldsymbol{U}_e+\boldsymbol{U}_w=(u_g,v_g)+(u_e,v_e)+(u_w,v_w). \tag{1}$$

3.2. Classical Currents Without Wave Effects

In this part, we use the Aviso MADT, QuickSCAT wind stress satellite data, and a physically based statistical model to calculate the classical ocean surface currents without waves, which contains geostrophic currents and classical Ekman currents corresponding to $\boldsymbol{U}_g+\boldsymbol{U}_e$ in equation (1). Following the method of *Lagerloef et al*. [1999], the momentum equations (detailed steps to derive the equations see Appendix A) of the linear steady balance are expressed as

$$-fh_{md}v_c=-gh_{md}\frac{\partial\xi}{\partial x}+\frac{\tau_x}{\rho_w}-ru_e, \tag{2}$$

$$fh_{md}u_c = -gh_{md}\frac{\partial \xi}{\partial y} + \frac{\tau_y}{\rho_w} - rv_e, \tag{3}$$

where f is the Coriolis parameter and $f = 2\Omega\sin\varphi$, in which $\Omega = 7.272 \times 10^{-5}$ rad/s, φ is the angle of latitude. ρ_w is the water density and $\rho_w = 1.02 \times 10^3$ kg/m^3, g is the gravitational acceleration that equal to 9.8 m/s^2, $(\partial\xi/\partial y, \partial\xi/\partial x)$ are the SSH gradients estimated from the Aviso MADT data. τ_x and τ_y are the zonal and meridional wind stress components from the QuickSCAT observations, (u_e, v_e) are the Ekman velocity, r is the frictional coefficient, h_{md} is the mixing depth, the values of r and h_{md} follow the regression analysis of *Lagerloef et al*. [1999], who find that $r = 2.15 \times 10^{-4}$ m/s and $h_{md} = 32.5$ m and remains fairly constant over the tropical band, we applied these values in our global analysis here. $\boldsymbol{U}_c = (u_c, v_c)$ represents the classical ocean surface currents vector, which can be divided into geostrophic currents $\boldsymbol{U}_g$ and classical Ekman currents $\boldsymbol{U}_e$

$$\boldsymbol{U}_c = (u_c, v_c) = \boldsymbol{U}_g + \boldsymbol{U}_e = (u_g, v_g) + (u_e, v_e). \tag{4}$$

Combining equations (2)–(4), we can obtain the geostrophic currents outside the equatorial band (5° S–5° N) as

$$u_g = -\frac{g}{f}\frac{\partial \xi}{\partial y}, \quad v_g = \frac{g}{f}\frac{\partial \xi}{\partial x}. \tag{5}$$

As for classical Ekman currents $\boldsymbol{U}_e$ in equation (4), in different regions, in an effort to account for the local wind-driven part of the velocity, both *Van Meurs and Niiler* [1997] and *Lagerloef et al*. [1999] have proposed a two parameter regression model between wind-driven Ekman current $\boldsymbol{U}_e$ and the surface wind stress as shown in equation (6)

$$\boldsymbol{U}_e = Be^{i\theta}(\tau_x + i\tau_y), \tag{6}$$

here, B is the amplitude coefficient, θ is the turning angle relative to the wind direction. In the region between 25° S and 25° N, *Lagerloef et al*. [1999] derived that B and θ vary with latitude according to the equations:

$$B = \frac{1}{\rho_w\sqrt{r^2 + f^2h_{md}^2}}, \quad \theta = \arctan\left(\frac{fh_{md}}{r}\right). \tag{7}$$

While in the region away from 25°S to 25°N, we take the method of *Sudre and Morrow* [2008], who regard both B and θ as constants as $B = 0.3$ ms^{-1}Pa^{-1}, $\theta = \pm 55°$, that is, 55° to right (left) of the wind in the northern (southern) hemisphere. The variations of parameters B and θ with latitude can be seen clearly in Figure 2, which show a jump at 25° latitude. It is induced by the different algorithms we applied in the tropical and subtropical regions and needs further improvement in the future study, which is beyond the scope of this study. Moreover, the turning angle θ at the sea surface is caused by the Coriolis force, at the equator where $f = 0$, there is no deflection of the current to the prevailing wind stress. Note that regression can only extract the component which has been included in the equation of the regression. Although the Lagrangian drifter velocity includes both classical Ekman current and the Stokes drift, regression equation (7) represents only the first part of it, which means equation (7) can only extract the component of classical Ekman part of the drifter velocity. The papers of *Sudre and Morrow* [2008] and *Sudre et al*. [2013] have used the same method to calculate the classical Ekman currents as well.

3.3. Wave-Modified Term

Classical Ekman model does not consider the wave-induced Coriolis-Stokes forcing, which are taken into account in this part. A wave-affected Ekman model and the ECMWF surface wave data are used to estimate the Stokes drift and wave-modified term. The momentum equations describing the unsteady state, ageostrophic current in the surface Ekman-Stokes layer are [*Jenkins*, 1989; *Rascle et al*., 2006; *Tang et al*., 2007]

$$\frac{\partial \boldsymbol{U}_{WE}}{\partial t} + if\boldsymbol{U}_{WE} = \frac{\partial}{\partial z}\left(A_z\frac{\partial \boldsymbol{U}_{WE}}{\partial z}\right) - if\boldsymbol{U}_s - \boldsymbol{T}_{wds}, \tag{8}$$

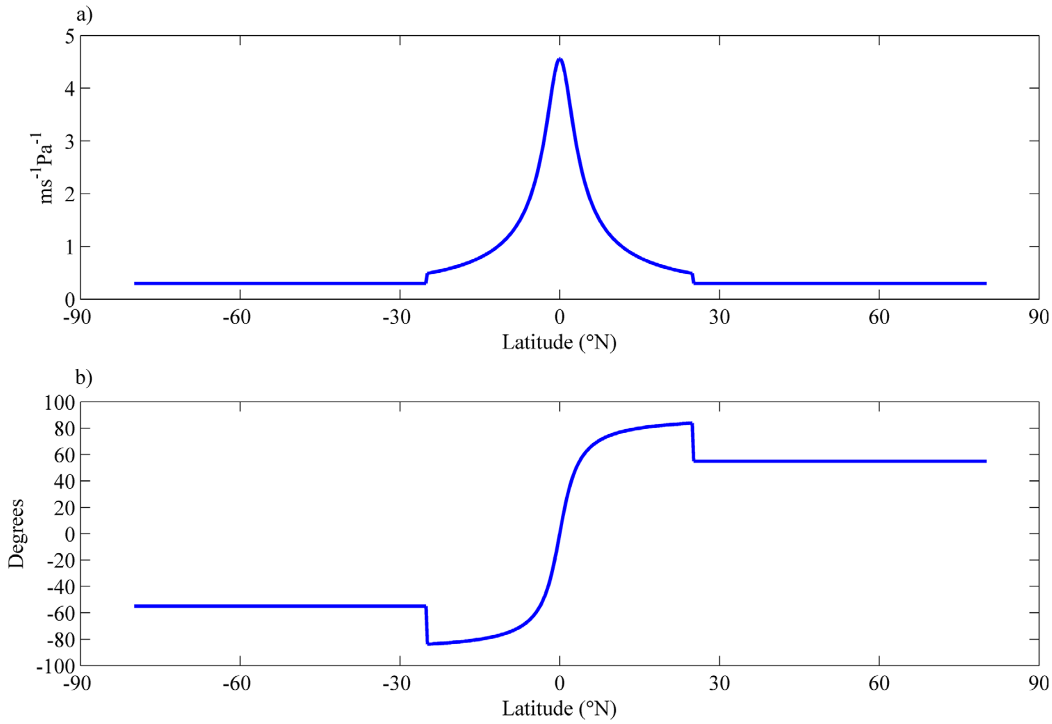

Figure 2. (a) The amplitude coefficient B. (b) The turning angel of Ekman currents relative to the wind direction (to right of the wind).

$$A_z \frac{\partial \boldsymbol{U}_{WE}}{\partial z} = \frac{\tau - \tau_{in}}{\rho_w}, \quad z=0, \tag{9}$$

$$\boldsymbol{U}_{WE} \to 0, \quad z \to -\infty, \tag{10}$$

where $\boldsymbol{U}_{WE}=(u_{WE}, v_{WE})$ is the wave-modified Ekman current, $\boldsymbol{U}_s$ is the Stokes drift vector, $\boldsymbol{T}_{wds}$ is the wave-induced momentum transfer from waves to mean flow due to dissipation of wave energy, $\tau=(\tau_x, \tau_y)$ is the surface wind stress, and τ_{in} is the reduction of wind stress due to wave generation. In this paper, we take $\boldsymbol{T}_{wds}=\tau_{in}=0$ and the equations (8)–(10) reduce to those of *Lewis and Belcher* [2004], which only includes the effect of Stokes drift. A_z is the vertical eddy viscosity, many methods have been taken to estimate the value of A_z, and different parameterizations have been proposed, a collection of values and functional forms can be found in *Huang* [1979] and *Santiago-Mandujano and Firing* [1990]. In this paper, we use the value independent of depth. The relationship between A_z and the wind speed $\boldsymbol{U}_{10}$ was first proposed by *Ekman* [1905] and then confirmed by *Santiago-Mandujano and Firing* [1990] as $A_z=1.2\times10^{-4}\boldsymbol{U}_{10}^2=1.2\times10^{-4}(u_{10}^2+v_{10}^2)$, u_{10} and v_{10} are the zonal and meridional wind speed components from QuickSCAT data in this paper. This method was also used by *Song* [2009] when considering depth independent eddy viscosity. For a monochromatic deep water wave with wave amplitude a, wave number k, and wave frequency σ, the Stokes drift $\boldsymbol{U}_s$ in related with such a wave is given by *Philipps* [1977]:

$$\boldsymbol{U}_s = U_s e^{2kz} \hat{\boldsymbol{k}}, \quad U_s = a^2 \sigma k, \tag{11}$$

in which U_s is the Stokes drift velocity at the sea surface, $\hat{\boldsymbol{k}}$ is the unit wavenumber vector. On the basis of the deep water dispersion relation $\sigma=\sqrt{gk}=\frac{2\pi}{T}$, we get that

$$k = \frac{4\pi^2}{gT^2}, \tag{12}$$

in which T represents the mean wave period provided by ECMWF data. Combined with equation (11), using the modeled significant wave height H_s ($a=\frac{1}{2}H_s$) and mean wave direction θ from ECMWF, we derive the following equations:

$$\hat{\boldsymbol{k}} = \sin\theta + i\cdot\cos\theta, \tag{13}$$

$$\boldsymbol{U}_s = \frac{2\pi^3 H_s^2}{gT^3}\cdot e^{\frac{8\pi^2}{gT^2}z}\cdot(\sin\theta + i\cdot\cos\theta),\ \ U_s = \frac{2\pi^3}{g}\frac{H_s^2}{T^3}. \tag{14}$$

Combining equations (8)–(14), *Liu et al*. [2007], *Polton et al*. [2005], and *Wu and Liu* [2008] have studied that the steady solution ($\frac{\partial \boldsymbol{U}_{WE}}{\partial t} = 0$) to equation (8) can be written as

$$\boldsymbol{U}_{WE} = \boldsymbol{W}_{e1} + \boldsymbol{W}_{es} + \boldsymbol{W}_s, \tag{15}$$

$$\boldsymbol{W}_{e1} = \frac{\tau}{\rho_w A_z j}e^{jz},\ \ \boldsymbol{W}_{es} = -\frac{2kj\boldsymbol{U}_s(0)}{(2k)^2 - j^2}\cdot e^{jz},\ \ \boldsymbol{W}_s = \frac{j^2\boldsymbol{U}_s(0)}{(2k)^2 - j^2}e^{2kz}, \tag{16}$$

$$\boldsymbol{U}_w = \boldsymbol{W}_{es} + \boldsymbol{W}_s, \tag{17}$$

where $\boldsymbol{W}_{e1}$ is the classical Ekman current velocity decreasing with depth, $\boldsymbol{W}_{es}$ and $\boldsymbol{W}_s$ are the two new terms in related with the Coriolis-Stokes forcing, $\boldsymbol{U}_w$ represents the modification of wind-generated surface waves to the classical Ekman solution. This modified term depends on the choice of Stokes drift $\boldsymbol{U}_s$ and the eddy viscosity A_z, $j = (1+i)/d$, $d = \sqrt{2A_z/f}$. Equation (16) is not applicable at the equator where $f = 0$. In the following, we only consider areas outside the equatorial band.

3.4. Wave-Modified Ocean Surface Currents

From the models described in sections 3.2–3.3, considering the impact of waves, we conclude that the wave-modified ocean surface currents are expressed as

$$\boldsymbol{U} = \boldsymbol{U}_c + \boldsymbol{U}_w = \boldsymbol{U}_g + \boldsymbol{U}_e + \boldsymbol{U}_w, \tag{18}$$

in which $\boldsymbol{U}_g$ and $\boldsymbol{U}_e$ are the geostrophic currents and classical Ekman currents estimated from Aviso MADT and QuickSCAT wind stress data, respectively, $\boldsymbol{U}_w$ is the wave-modified term estimated from ECMWF parameters (mean wave direction, mean wave period, and significant wave height). As for the classical Ekman currents in this study, as we do not need to use value at a fixed depth like $\boldsymbol{W}_{e1}$, instead, we use the Ekman current representing 15 m depth averaged over some depth as is in section 3.2, which can better express the motion of Lagrangian drifters drogued at 15 m depth. Then the four products described in the introduction part can be easily obtained. That is, the classical ocean surface currents ($\boldsymbol{U}_g + \boldsymbol{U}_e$), wave-modified products ($\boldsymbol{U}_g + \boldsymbol{U}_e + \boldsymbol{U}_w$), OSCAR currents (without waves), and wave-modified OSCAR currents (OSCAR + $\boldsymbol{U}_w$).

4. Results and Analysis

In this study, we use the Aviso SSH, QuikSCAT wind stress satellite data, and ECMWF Interim surface wave data sets of 2000–2008 to retrieve the ocean surface currents of the global ocean. All of these data sets are sampled daily and gridded with the resolution 0.25° × 0.25°. To assess the quality of our retrieving flow and the relative importance of surface waves on the ocean surface currents, the results of the above referred four products (described in the introduction and section 3.4) are compared with in situ Lagrangian drifter currents to verify whether the surface waves will have positive effects on the surface currents.

4.1. Assessment of Wave Influences

Using QuikSCAT wind speed and ECMWF surface wave data sets, combined with equations (8)–(17), we can compute the modification of wind-generated surface waves to the wind-driven classical Ekman solution that does not consider the effects of surface waves. The distributions of 9 year averaged wave-modified term, together with its zonal average and the corresponding wind speed components are shown in Figure 3, from which we can see that the wave-modified term is very strong in mid and high latitudes, especially in the Southern Ocean region because of the westerly wind there. From Figures 3a1 and 3b1, we can find that the pattern of zonal component of wave-modified term is similar to that of the wind speed, the same result for value of the vector can also be found in Figure 3c. This suggests that the magnitude of the Stokes drift or the wave-modified term is directly in related with the strength of the surface wind, the wave-modified term is especially large in strong wind areas.

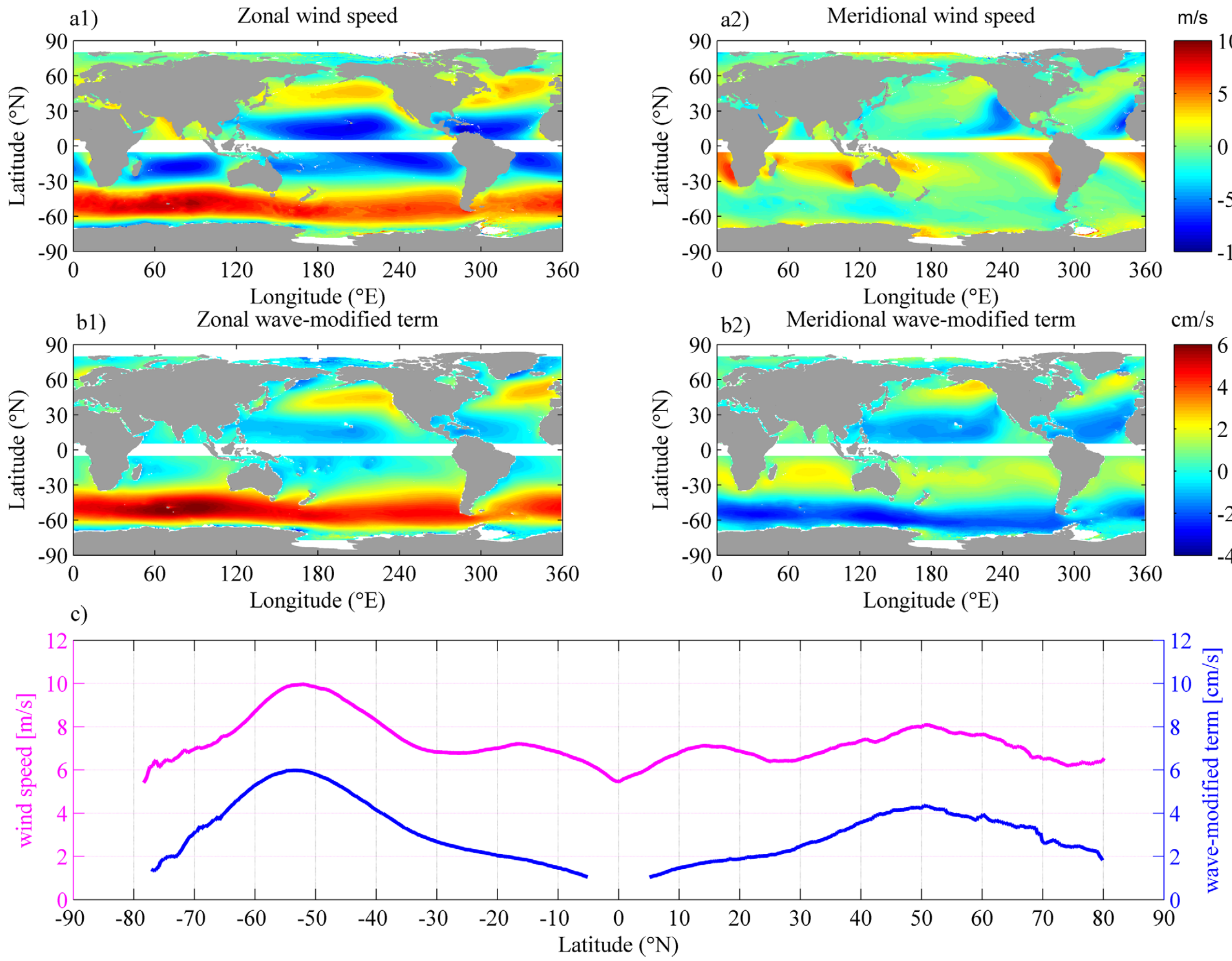

Figure 3. Global distributions of (a1) zonal wind speed and (a2) meridional wind speed, (b1) zonal component of the wave-modified term and (b2) meridional component of the wave-modified term. (c) Zonal average of the wind speed (red line) and wave-modified term (blue line). These figures are all for the year 2000–2008 over 0.25° × 0.25° grid.

In order to estimate the contributions of waves (Stokes drift here) to surface currents, the ratio of the wave-modified term to total currents is calculated (Figure 4a). The ratio surpasses 0.2 accounts for most of the global ocean. In mid and high latitudes of the North Pacific and in the Southern Ocean region, the ratio is in the interval 0.2–0.4, some even exceeds 0.5 and approaches 0.6. The zonal profile is shown in Figure 4b which can show the same phenomenon. Figure 5a shows the angle between wind stress and the wave-modified term, positive (negative) values indicate that the wave-modified term turns to right (left) of the wind. Note that the angle here is different from the turning angle presented in Figure 2b, which represents the turning angle of classical Ekman currents relative to the wind direction. Figure 5b is the zonal average of Figure 5a and presents that the wave-modified term turns to left (right) of the wind in the southern (northern) hemisphere, which is consistent with the result of *Wu and Liu* [2008]. It also shows that in strong waves affected area, the angles between the two are much smaller. These results support that the wave-induced Coriolis-Stokes forcing makes a significant contribution to ocean surface currents. Just like Ekman currents and geostrophic currents, the Stokes drift is coordinately important, it cannot be neglected and should be considered as the third term when retrieving ocean surface currents, especially in mid and high latitudes.

4.2. Comparison With OSCAR Currents and Drifter Observations

To assess the quality of the retrieved currents, any satellite-derived product has to be validated. This wave-modified one is to be validated by comparing with other satellite current products and in situ observations.

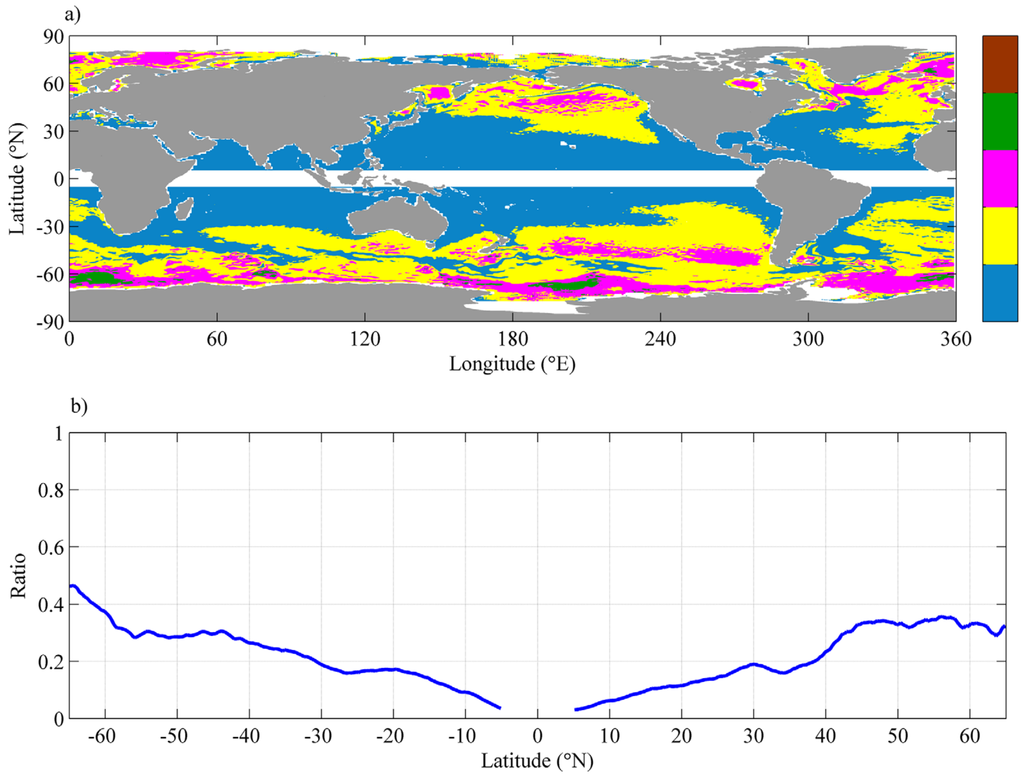

Figure 4. (a) Ratio of the wave-modified term to total ocean surface currents (wave-modified term/total ocean surface currents) over the period 2000–2008 with the spatial resolution 0.25° × 0.25°. (b) Zonal profile of the ratio.

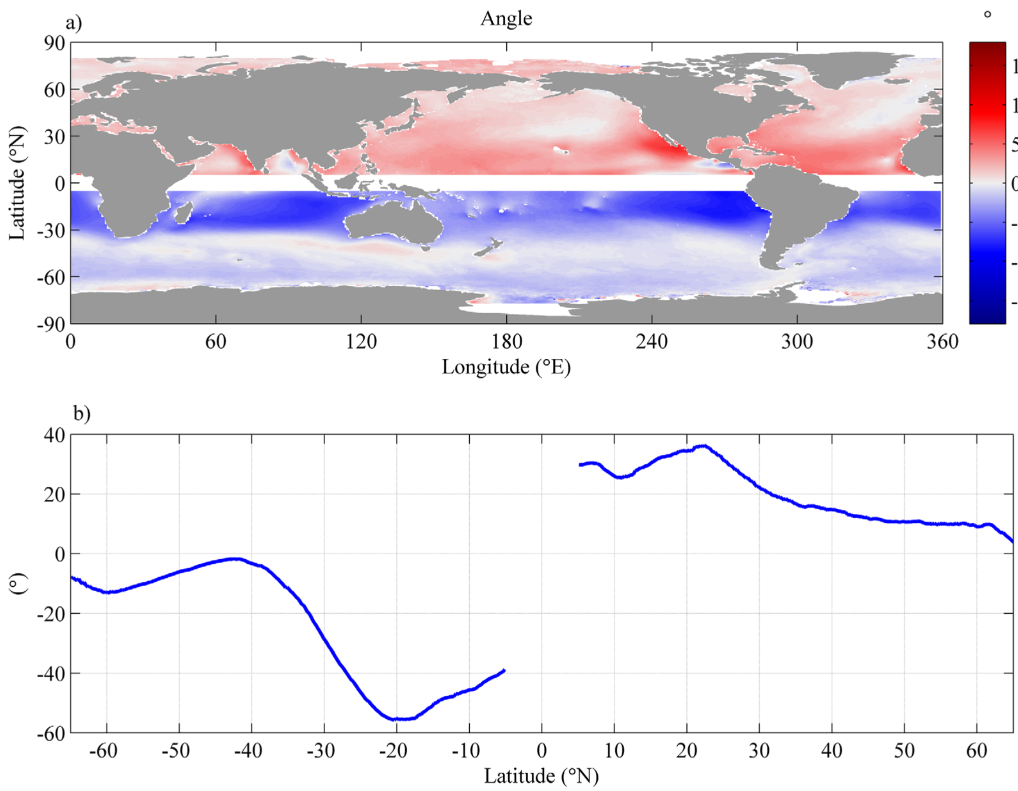

Figure 5. (a) Angles between wind stress and the wave-modified term. (b) Zonal average of angles in (a).

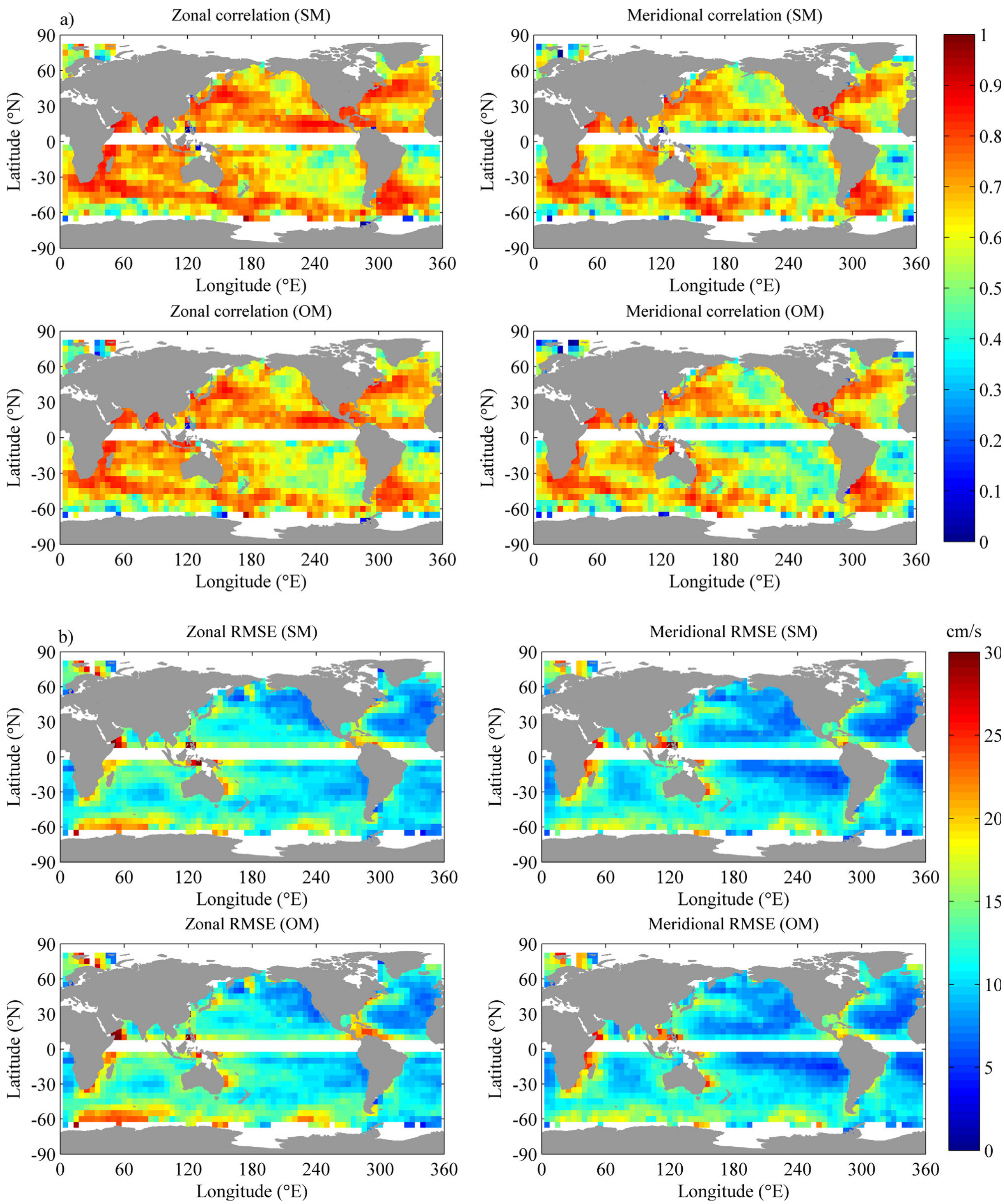

Figure 6. Spatial distributions of the correlations between zonal and meridional (a) top two plots: wave-modified satellite-derived ocean surface currents (SM) and in situ Lagrangian drifter currents, bottom two plots: wave-modified OSCAR currents (OM) and in situ Lagrangian drifter currents and (b) the corresponding root mean square error (RMSE) as indicated over 5° × 5°. In each grid point, only observations that are longer than seven numbers are used here.

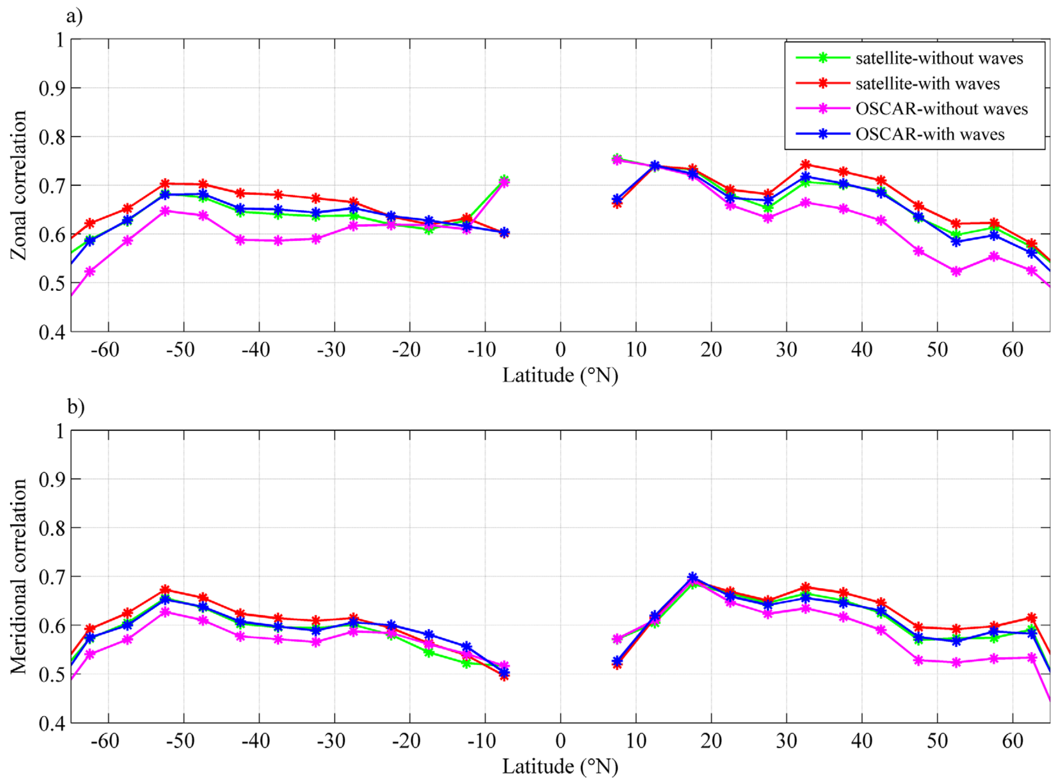

Figure 7. Zonal averages of (a) zonal correlations between zonal component of the satellite-derived currents and zonal component of the Lagrangian drifter currents. (b) Meridional correlations between meridional component of the satellite-derived currents and meridional component of the Lagrangian drifter currents.

In this study, the validations are performed using OSCAR products and all the available Lagrangian drifter data of the global ocean for the year 2000–2008. As OSCAR currents are temporally averaged on a 10 day time scale, and provided on a 5 day time resolution, while our satellite-derived currents and the wave-modified term are daily products, before validation, we averaged our currents with or without waves and the wave-modified term to have the same temporal resolution as OSCAR ones. As the wave-modified products of this paper are gridded with the spatial resolution $0.25° \times 0.25°$, before validation, some measures have to be taken. For each drifter current vector, taking into account the position and time, we use a spatial bilinear interpolation and a temporal linear interpolation to interpolate the gridded zonal and meridional components of our currents and the OSCAR products onto each 6 h in situ drifter point, respectively. To present the global distributions of our comparison results, we have binned all the data into $5° \times 5°$ resolution boxes from 1 January 2000 to 31 December 2008 [*Sudre and Morrow*, 2008].

Figure 6 shows global distributions of the correlation and root mean square error (RMSE) between wave-modified currents and Lagrangian drifter currents, available during the period 2000–2008. We find that in most of the oceans, both for zonal and meridional currents, the correlations between our wave-modified products and the drifter currents are larger than that between wave-modified OSCAR currents and drifter currents, while the RMSE is much smaller. That means the quality of our wave-modified product is better adapted to the in situ drifter currents than OSCAR currents.

To estimate the relative importance of wave-induced Coriolis-Stokes forcing on the surface currents, we compare the currents that include Stokes drift with currents that do not include it. Here we give zonal profile of the zonal and meridional correlations and RMSE for each current product as shown in Figures 7 and 8. To remove the influence of sea ice, we only consider areas between 65°S and 65°N. Figure 7 shows that outside the equatorial band of 10°S–10°N, both for zonal and meridional currents, our products or OSCAR currents considering the impact of waves show a consistent higher correlation with the drifter currents compared with currents without waves (red and blue lines versus green and pink lines). We can see that our satellite-derived currents accompanied with the surface waves have the highest correlation. From

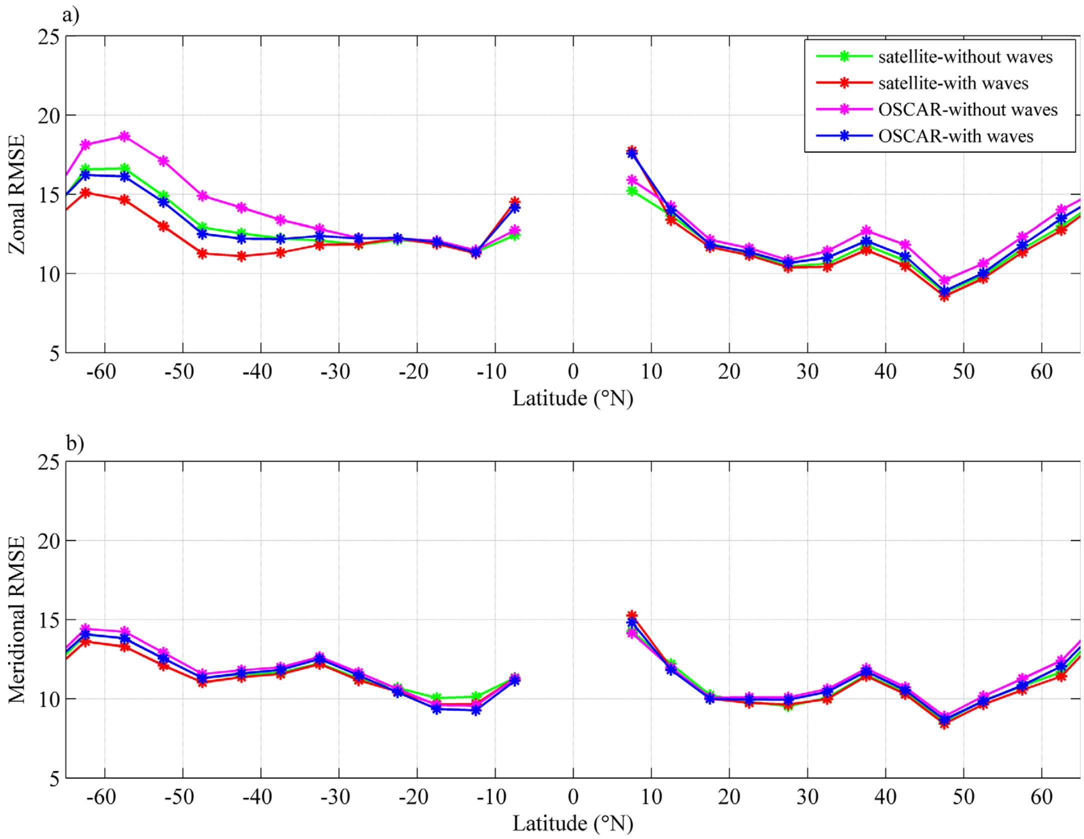

Figure 8. Zonal averages of (a) zonal RMSE between zonal component of the satellite-derived currents and zonal component of the Lagrangian drifter currents. (b) Meridional RMSE between meridional component of the satellite-derived currents and meridional component of the Lagrangian drifter currents.

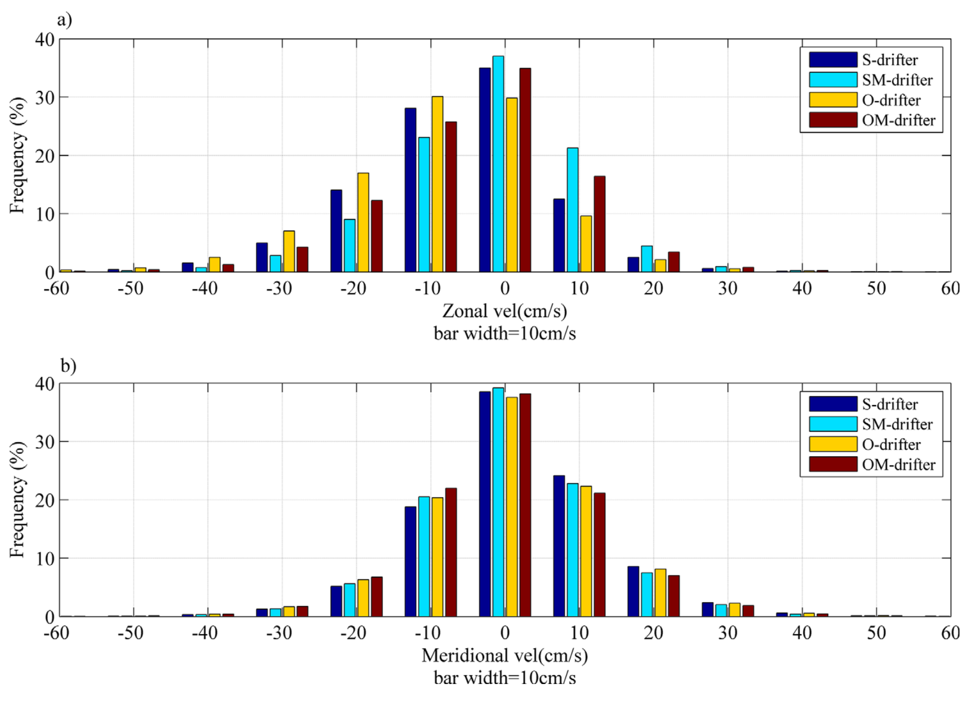

Figure 9. Histograms of the difference between gridded ocean surface currents with or without waves and drifter data. (a) Zonal component. (b) Meridional component. S indicates the satellite-derived currents without waves, SM indicates the surface currents with waves. O indicates the OSCAR currents without waves, OM indicates the OSCAR currents with waves.

Table 1. Statistical Analysis of the Retrieved Currents and the Lagrangian Drifter Currents in the Southern Ocean

	Correlation				RMSE			
	Satellite-Drifter	SM-Drifter	OSCAR-Drifter	OM-Drifter	Satellite-Drifter	SM-Drifter	OSCAR-Drifter	OM-Drifter
Zonal	0.73	0.75	0.68	0.72	14.00	12.36	15.94	13.65
Meridional	0.69	0.71	0.67	0.69	12.15	11.83	12.48	12.19

Figure 8, we come to the conclusion that the RMSE between our wave-modified satellite-derived currents and the in situ data are much smaller than the other products. The relatively lower correlation and higher RMSE for OSCAR at mid to high latitudes may be affected by its 1/3° spatial resolution and the limited spatial resolution of T/P and Jason altimetric observations, which misses much of the mesoscale eddy energy at these latitudes. Following the analysis of *Sudre and Morrow* [2008], our geostrophic currents derived from the Aviso MADT data are global and maintains high spatial resolution (1/4°), whereas OSCAR geostrophic currents are spatially smoothed to obtain their 1/3° product. Though adequate for the tropics, our results show that it is important to maintain the 1/4° spatial resolution at mid to high latitudes, where the Rossby radius scales are small and any small scales changes will be amplified by the geostrophic currents. Furthermore, the coarse temporal resolution of 5 days may also be influential compared with the daily data of our product. While in the equatorial band, the OSCAR product shows some higher correlation and lower RMSE with the drifter currents. This confirms that the diagnostic model of the method proposed by *Bonjean and Lagerloef* [2002] has improved to be better adapted to the tropical Pacific than the *Lagerloef et al*. [1999] algorithm which only calculates geostrophic currents and Ekman currents in our product.

To better quantify the importance of wave-induced Coriolis-Stokes forcing on surface currents and the differences between our products and OSCAR currents, we have chosen strong wind areas of the Southern Ocean (40° S-65° S), where the prevailing westerly winds generate strong Ekman currents and large ocean

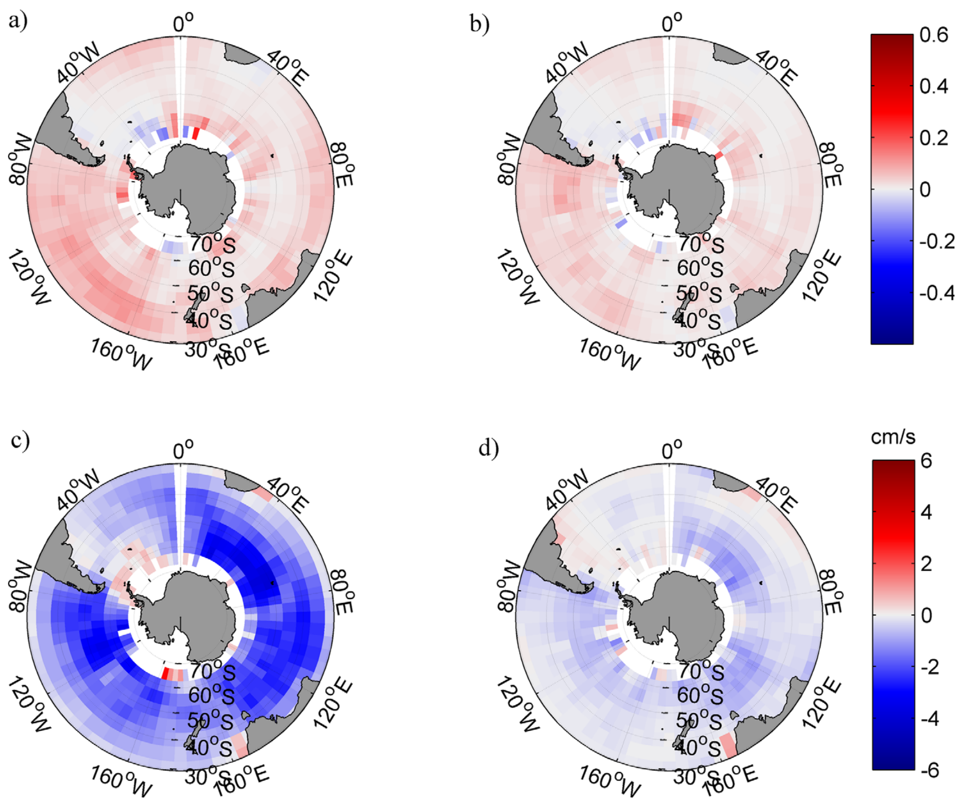

Figure 10. (a) Zonal correlation after modified–zonal correlation before modified. (b) the same as Figure 10a, but for the meridional correlation difference. (c) The same as Figure 10a, but for the zonal RMSE difference. (d) The same as Figure 10b, but for the meridional RMSE difference.

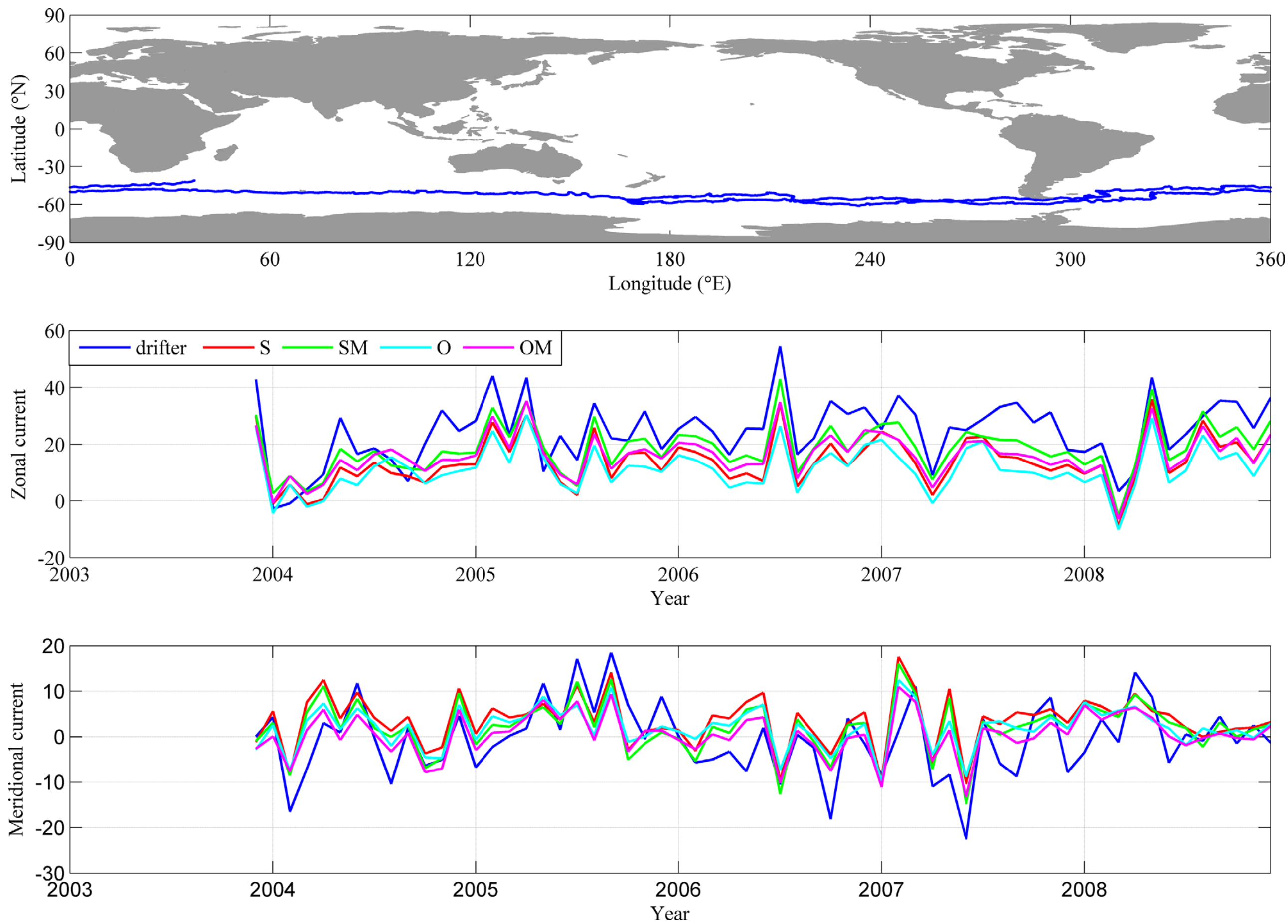

Figure 11. (a) Trajectory of the 41284 drifter. (b) Time series of the zonal current. (c) Time series of the meridional current.

surface waves associated with the Stokes drift. We show histograms of differences between our satellite-derived currents, as well as OSCAR currents with or without waves and the Lagrangian drifter currents both in zonal and meridional components (Figure 9), 108,143 profiles in total. We find that considering the effects of surface waves, the zonal and meridional percentages of the differences approaching zero are higher compared with currents without waves both for our products and OSCAR currents. Moreover, the percentage of our products is a little higher than OSCAR ones. A statistical analysis is formed in Table 1. Considering the impact of surface waves, the correlation in the Southern Ocean has slightly improved from 0.73 (0.69) to 0.75 (0.71) in zonal and meridional component, respectively. Simultaneously, the RMSE in the same area has improved from 14.00 (12.15) to 12.36 (11.83). As a contrast, the correlation between OSCAR currents and the Lagrangian drifter velocity has improved from 0.68 (0.67) to 0.72 (0.69) and the RMSE has decreased from 15.94 (12.48) to 13.65 (12.19) in zonal and meridional components. Considering the impact of the Stokes drift, the correlation (RMSE) between our products and the drifter currents is higher (lower) than the correlation (RMSE) of OSCAR ones, which means that our wave-modified currents can better express the ocean circulation than OSCAR currents.

Table 2. Statistical Analysis of the Retrieved Currents and the Lagrangian Drifter Currents for the 41284 Drifter in the Southern Ocean

	Correlation				RMSE			
	Satellite-Drifter	SM-Drifter	OSCAR-Drifter	OM-Drifter	Satellite-Drifter	SM-Drifter	OSCAR-Drifter	OM-Drifter
Zonal	0.79	0.81	0.75	0.79	17.86	15.05	20.37	17.19
Meridional	0.77	0.79	0.75	0.77	14.50	13.77	14.93	14.35

Figure 10 also sustains the point, from which we can see that in the Southern Ocean region, the wave-modified correlation (RMSE) increases (decreases) almost everywhere except for a few points. To give detailed analysis of the wave effects, we select a drifter of the Southern Ocean with the ID number 41284, it has 7357 current profiles and the operating date is from 19 December 2003 to 31 December 2008. The drifter's trajectory and time series are shown in Figure 11. It shows that surface currents considering the impact of waves show the best consistency with in situ drifter observations, comparing with those like currents without waves, OSCAR currents with and without waves. The correlation coefficient and RMSE analysis of the single drifter are shown in Table 2, which presents higher correlation and lower RMSE with drifter currents after taking waves into account.

5. Summary and Conclusions

In this paper, the function of Stokes drift on ocean surface currents is investigated by incorporation of the wave-induced Coriolis-Stokes forcing into the classical Ekman model [*Wu and Liu*, 2008]. *Polton et al*. [2005] showed that the Coriolis-Stokes forcing plays a significant role in determining the current profile of the Ekman-Stokes layer [*Liu et al*., 2007]. As the Ekman current constitutes an important part of the surface current, then whether the Stokes drift can improve the surface current profile of the global ocean needs to be studied. What we emphasize in this paper is the wave-added work on surface currents and compare the result with OSCAR and in situ Lagrangian drifter currents as well.

Ocean surface currents considering the impact of waves contain three components, the Ekman currents from wind stress, the geostrophic currents from SSH, and the Stokes drift estimated from the surface wave data. Using the ECMWF surface wave and QuikSCAT surface wind data of 2000–2008, we estimate that about 67% (74%) of the zonal (meridional) surface currents have been improved of the global ocean, indicating the importance of waves in driving and maintaining the oceanic general circulation. The percentages are even much larger in the Southern Ocean (40°S–65°S) with 90% and 91%, which indicates that the wave-induced Coriolis-Stokes forcing is most significant within the Southern Ocean. It proves that the traditional methods of retrieving surface currents using satellite data are not perfect, it should consider the wave effects.

From the results in this study, we believe that the incorporation of waves would be effective in improving the satellite-derived ocean surface currents, especially in the Southern Ocean, it should be considered to account for one important part of ocean surface currents estimated from the satellite data.

Appendix A: Linear Steady Balance Equations Procedure

This appendix describes detailed steps to derive equations (2) and (3). We take the method proposed by *Bonjean and Lagerloef* [2002], who consider a linear and steady flow in a surface layer where the horizontal velocity $\boldsymbol{U} = (u, v)$ is varying with depth z. Ignoring the effects of sea surface temperature, the basic equations are

$$if\ \boldsymbol{U} = -\frac{1}{\rho_w}\nabla p + A_z\frac{\partial}{\partial z}\left(\frac{\partial \boldsymbol{U}}{\partial z}\right), \tag{A1}$$

$$\frac{1}{\rho_w}p_z = -g, \tag{A2}$$

subjecting to the following boundary conditions:

$$A_z\frac{\partial \boldsymbol{U}}{\partial z}\bigg|_{z=0} = \frac{\boldsymbol{\tau}}{\rho_w}, \tag{A3}$$

$$\boldsymbol{U}'(z=-H) = 0, \tag{A4}$$

where f is the Coriolis parameter and $f = 2\Omega\sin\varphi$, in which $\Omega = 7.272 \times 10^{-5}$ rad/s, φ is the angle of latitude. ρ_w is the water density and $\rho_w = 1.02 \times 10^3$ kg/m^3, $\nabla = \partial/\partial x + i\partial/\partial y$, p is the pressure, g is the gravitational acceleration that equal to 9.8 m/s^2. $\boldsymbol{\tau} = \tau_x + i\tau_y$ represents the surface wind stress, A_z denotes the vertical eddy viscosity, when A_z is depth independent, we use the relationship between A_z and the wind speed $\boldsymbol{U}_{10}$ first proposed by *Ekman* [1905] and then confirmed by *Santiago-Mandujano and Firing* [1990] as $A_z = 1.2\times10^{-4}\boldsymbol{U}_{10}^2$.

Hereafter we denote ξ as the water level above the sea surface (sea surface height), define $\boldsymbol{U}_c$ as the velocity averaged between the interface and the mixing depth h_{md}, we have

$$\boldsymbol{U_c} = \frac{1}{h_{md}}\int_{-h_{md}}^{0}\boldsymbol{U}(z)dz, \tag{A5}$$

where $\boldsymbol{U}_c = (u_c, v_c)$ represents the classical ocean surface currents vector, which is the sum of geostrophic currents $\boldsymbol{U}_g$ and classical Ekman currents $\boldsymbol{U}_e$. Then Combining equations (A1)–(A5), we get that

$$if\ \ \boldsymbol{U_c} = \frac{if}{h_{md}}\int_{-h_{md}}^{0}\boldsymbol{U}(z)\mathrm{d}z = -g\nabla\xi + \frac{\boldsymbol{\tau} - \rho_w A_z \boldsymbol{U'_c}(-h_{md})}{\rho_w h_{md}}, \tag{A6}$$

replaced $A_z\boldsymbol{U}'_c(-h_{md})$ by a Rayleigh friction term $r\boldsymbol{U}_e$ [*Bonjean and Lagerloef*, 2002], where r is the frictional coefficient, both r and h_{md} in the study follow the analysis of *Lagerloef et al*. [1999], who find that $r = 2.14 \times 10^{-4}$ m/s and $h_{md} = 32.5$ m and remains fairly constant over the tropical band, we applied these values in our global analysis here. Equation (A6) can be rewritten as

$$if(u_c + iv_c) = -g\left(\frac{\partial\xi}{\partial x} + i\frac{\partial\xi}{\partial y}\right) + \frac{\boldsymbol{\tau} - \rho_w r\boldsymbol{U}_e}{\rho_w h_{md}}. \tag{A7}$$

Dividing equation (A7) into real and imaginary components, we get that

$$-fh_{md}v_c = -gh_{md}\frac{\partial\xi}{\partial x} + \frac{\tau_x}{\rho_w} - ru_e, \tag{A8}$$

$$fh_{md}u_c = -gh_{md}\frac{\partial\xi}{\partial y} + \frac{\tau_y}{\rho_w} - rv_e, \tag{A9}$$

which are the same forms as that in equations (2) and (3).

Acknowledgments
The authors were grateful for the comments by two anonymous reviewers. This work was supported by the National Natural Science Foundation of China (grant 41376028), the China 973 Project (grant 2012CB956000), the CAS (Chinese Academy of Sciences) "100 Talent" Program (grant Y32109101L), the open **Foundation of State Key Laboratory of Remote Sensing Science** (grant **OFSLRSS201504**), the **Leadership in Entrepreneurship and Innovation Awarded by Qingdao Municipal Government** (grant **13-CX-26**), the **NSFC-Shandong Joint Fund for Marine Science Research Centers** (grant **U1406401**), the **NSFC-Innovation research group of Sciences Fund** (grant **41421005**), and the **Natural Science Foundation of Shandong Province**, China (grant **ZR2014DQ027**). The QuikSCAT wind data were processed and distributed by the Centre ERS d'Archivage et de Traitement (CERSAT; http://cersat.ifremer.fr/) and could be downloaded from ftp://ftp.ifremer.fr/ifremer/cersat/products/gridded/MWF/L3/QuikSCAT/Daily. The global daily averaged SSH data were provided by the French Space Agency, Archiving, Validation, and Interpretation of Satellite Oceanographic Data (AVISO; http://aviso.altimetry.fr/index.phd?id=1271). The Interim surface wave data sets could be downloaded from the ECMWF link: http://apps.ecmwf.int/datasets/data/interim-full-daily/. The Ocean Surface Current Analyses Real-Time (OSCAR) data were obtained from the NASA Physical Oceanography DAAC (http://podaac.jpl.nasa.gov/) and developed by ESR, the data can be downloaded from http://www.oscar.noaa.gov/datadisplay/oscar_datadownload.php. In situ Lagrangian drifter data were provided by the Global Drifter Program (GDP; http://www.aoml.noaa.gov/phod/dac/index.php) and were downloaded from http://www.aoml.noaa.gov/envids/gld/dirkrig/parttrk_spatial_temporal.php.

References

Atlas, R., R. Hoffman, S. Bloom, J. Jusem, and J. Ardizzone (1996), A multiyear global surface wind velocity dataset using SSM/I wind observations, *Bull. Am. Meteorol. Soc.*, *77*(5), 869–882, doi:10.1175/1520-0477(1996)077<0869:AMGSWV>2.0.CO;2.

Bonjean, F., and G. S. Lagerloef (2002), Diagnostic model and analysis of the surface currents in the tropical Pacific Ocean, *J. Phys. Oceanogr.*, *32*(10), 2938–2954, doi:10.1175/1520-0485(2002)032<2938:DMAAOT>2.0.CO;2.

Cushman-Roisin, B. (1994), *Introduction to geophysical fluid dynamics*, 320 pp., Prentice-Hall, Englewood Cliffs, N. J.

Ekman, V. W. (1905), On the influence of the earth\'s rotation on ocean currents, *Ark. Mat. Astron. Fys.*, *2*, 1–53.

Hansen, D. V., and P.-M. Poulain (1996), Quality control and interpolations of WOCE-TOGA drifter data, *J. Atmos. Oceanic Technol.*, *13*(4), 900–909, doi:10.1175/1520-0426(1996)013<0900:QCAIOW>2.0.CO;2.

Hasselmann, K. (1970), Wave-driven inertial oscillations, *Geophys. Fluid Mech.*, *1*(3-4), 463–502, doi:10.1080/03091927009365783K.

Huang, N. E. (1979), On surface drift currents in the ocean, *J. Fluid Mech.*, *91*(01), 191–208, doi:10.1017/S0022112079000112.

Jenkins, A. D. (1987), Wind and wave induced currents in a rotating sea with depth-varying eddy viscosity, *J. Phys. Oceanogr.*, *17*(7), 938–951.

Jenkins, A. D. (1989), The use of a wave prediction model for driving a near-surface current model, *Dtsch. Hydrogr. Z.*, *42*(3–6), 133–149.

Johnson, E. S., F. Bonjean, G. S. E. Lagerloef, J. T. Gunn, and G. T. Mitchum (2007), Validation and Error Analysis of OSCAR Sea Surface Currents, *J. Atmos. Oceanic Techonol.*, *24*(4), 688–701, doi:10.1175/jtech1971.1.

Lagerloef, G. S., G. T. Mitchum, R. B. Lukas, and P. P. Niiler (1999), Tropical Pacific near-surface currents estimated from altimeter, wind, and drifter data, *J. Geophys. Res.*, *104*(C10), 23,313–23,326, doi:10.1029/1999JC900197.

Lewis, D., and S. Belcher (2004), Time-dependent, coupled, *Ekman* boundary layer solutions incorporating Stokes drift, *Dyn. Atmos. Oceans*, *37*(4), 313–351, doi:10.1016/j.dynatmoce.2003.11.001.

Liu, B., K. Wu, and C. Guan (2007), Global estimates of wind energy input to subinertial motions in the *Ekman*-Stokes layer, *J. Oceanogr.*, *63*(3), 457–466, doi:10.1007/s10872-007-0041-6.

Liu, Y., R. H. Weisberg, S. Vignudelli, and G. T. Mitchum (2014), Evaluation of altimetry-derived surface current products using Lagrangian drifter trajectories in the eastern Gulf of Mexico, *J. Geophys. Res. Oceans*, *119*, 2827–2842, doi:10.1002/2013JC009710.

Lumpkin, R., and M. Pazos (2007), Measuring surface currents with Surface Velocity Program drifters: The instrument, its data, and some recent results, *in Lagrangian Analysis and Prediction of Coastal and Ocean Dynamics*, edited by A. Griffa et al., chap. 2, pp. 39–67, Cambridge Univ. Press. Cambridge, U. K.

McWilliams, J. C., and J. M. Restrepo (1999), The wave-driven ocean circulation, *J. Phys. Oceanogr.*, *29*(10), 2523–2540, doi:10.1175/1520-0485(1999)029<2523:TWDOC>2.0.CO;2.

Niiler, P. P., and J. D. Paduan (1995), Wind-driven motions in the northeast Pacific as measured by Lagrangian drifters, *J. Phys. Oceanogr.*, *25*(11), 2819–2830.

Pazan, S. E., and P. P. Niiler (2001), Recovery of near-surface velocity from undrogued drifters, *J. Atmos. Oceanic Technol.*, *18*(3), 476–489.

Perrie, W., C. Tang, Y. Hu, and B. DeTracy (2003), The impact of waves on surface currents, *J. Phys. Oceanogr.*, *33*(10), 2126–2140, doi: 10.1175/1520-0485(2003)033<2126:TIOWOS>2.0.CO;2.

Philipps, O. (1977), *The Dynamics of the Upper Ocean*, 336 pp., Cambridge Univ. Press, Cambridge, U. K.

Polton, J. A., D. M. Lewis, and S. E. Belcher (2005), The role of wave-induced Coriolis-Stokes forcing on the wind-driven mixed layer, *J. Phys. Oceanogr.*, *35*(4), 444–457, doi:10.1175/JPO2701.1.

Price, J. F., and M. A. Sundermeyer (1999), Stratified *Ekman* layers, *J. Geophys. Res.*, *104*(C9), 20,467–20,494, doi:10.1029/1999JC900164.

Rascle, N., F. Ardhuin, and E. A. Terray (2006), Drift and mixing under the ocean surface: A coherent one-dimensional description with application to unstratified conditions, *J. Geophys. Res.*, *111*, C03016, doi:10.1029/2005JC003004.

Reynolds, R. W., N. A. Rayner, T. M. Smith, D. C. Stokes, and W. Wang (2002), An improved in situ and satellite SST analysis for climate, *J. Clim.*, *15*(13), 1609–1625, doi: 10.1175/1520-0442(2002)015<1609:AIISAS>2.0.CO;2.

Santiago-Mandujano, F., and E. Firing (1990), Mixed-layer shear generated by wind stress in the central equatorial Pacific, *J. Phys. Oceanogr.*, *20*(10), 1576–1582, doi:10.1175/1520-0485(1990)020<1576:MLSGBW>2.0.CO;2.

Sikhakolli, R., R. Sharma, R. Kumar, B. S. Gohil, A. Sarkar, K. V. S. R. Prasad, and S. Basu (2013), Improved determination of Indian Ocean surface currents using satellite data, *Remote Sens. Lett.*, *4*(4), 335–343, doi:10.1080/2150704x.2012.730643.

Song, J.-B. (2009), The effects of random surface waves on the steady Ekman current solutions, *Deep Sea Res., Part I*, *56*(5), 659–671, doi: 10.1016/j.dsr.2008.12.014.

Stokes, G. G. (1847), On the theory of oscillatory waves, *Trans. Cambridge Philos. Soc.*, *8*, 441–473.

Sudre, J., and R. A. Morrow (2008), Global surface currents: A high-resolution product for investigating ocean dynamics, *Ocean Dyn.*, *58*(2), 101–118, doi:10.1007/s10236-008-0134-9.

Sudre, J., C. Maes, and V. Garcon (2013), On the global estimates of geostrophic and Ekman surface currents, *Limnol. Oceanogr. Methods*, *3*(0), 1–20, doi:10.1215/21573689-2071927.

Tang, C., W. Perrie, A. Jenkins, B. DeTracey, Y. Hu, B. Toulany, and P. Smith (2007), Observation and modeling of surface currents on the Grand Banks: A study of the wave effects on surface currents, *J. Geophys. Res.*, *112*, C10025, doi:10.1029/2006JC004028.

Van Meurs, P., and P. P. Niiler (1997), Temporal variability of the large-scale geostrophic surface velocity in the Northeast Pacific, *J. Phys. Oceanogr.*, *27*(10), 2288–2297, doi:10.1175/1520-0485(1997)027<2288:TVOTLS>2.0.CO;2.

Wu, K., and B. Liu (2008), Stokes drift–induced and direct wind energy inputs into the Ekman layer within the Antarctic Circumpolar Current, *J. Geophys. Res.*, *113*, C10002, doi:10.1029/2007JC004579.

Erratum

In the originally published version of this article, a few instances of text were incorrectly typeset. The following have since been corrected, and this version may be considered the authoritative version of record. The names of the authors were changed to Zhenli Hui and Yongsheng Xu. In equation (14), $(\cos\theta + i \cdot \sin\theta)$ was changed to $(\sin\theta + i \cdot \cos\theta)$. In section 4.1, “right (left)” was changed to “left (right)”. Finally, Figure 3 has been revised so that the color key is the same in both Figures 3a and 3b. Also, in Figure 3c, the units of wind speed (pink line) and wave-modified term (blue line) in fact are not the same.